ORIGINAL ARTICLE

# $^1$H-NMR study of the metabolome of an exceptionally anoxia tolerant vertebrate, the crucian carp (*Carassius carassius*)

Isabelle Lardon · Göran E. Nilsson ·
Jonathan A. W. Stecyk · Trung Nghia Vu ·
Kris Laukens · Roger Dommisse · Gudrun De Boeck

**Abstract** The crucian carp (*Carassius carassius*) can tolerate anoxia for days to months, depending on the temperature. In this study, we applied $^1$H-NMR-based metabolomics to polar extracts of crucian carp brain, heart, muscle and liver samples obtained from fish exposed to either control normoxic conditions, acute anoxia (24 h), chronic anoxia (1 week) or reoxygenation (for 1 week following chronic anoxia) at 5 °C. Spectra of the examined tissues revealed changes in several energy-related compounds. In particular, anoxic stress resulted in decreased concentrations of phosphocreatine (muscle, liver) and glycogen (liver) and ATP/ADP (liver, heart and muscle) and increased concentrations of lactate (brain, heart, muscle) and beta-hydroxybutyric acid (all tissues). Likewise, increased concentrations of inhibitory compounds (glycine, gamma-amino butyric acid or GABA) and decreased concentrations of excitatory metabolites (glutamate, glutamine) were confirmed in the anoxic brain extracts. Additionally, a decrease of *N*-acetylaspartate (NAA), an important neuronal marker, was also observed in anoxic brains. The branched-chain amino acids (BCAA) valine/isoleucine/leucine increased in all anoxic tissues. Possibly, this general tissue increase can be due to an inhibited mitochondrial function or due to protein degradation/protein synthesis inhibition. In this study, the potential and strength of the $^1$H-NMR is highlighted by the detection of previously unrecognized changes in metabolites. Specifically, myo-inositol substantially decreased in the heart of anoxic crucian carp and anoxic muscle tissue displayed a decreased concentration of taurine, providing novel insights into the anoxia responses of the crucian carp.

**Keywords** Anoxia · Crucian carp · Metabolomics · NMR · Tissue extraction

I. Lardon · R. Dommisse · G. De Boeck
Departments of Chemistry and Biology, University of Antwerp, Groenenborgerlaan 171, 2020 Antwerp, Belgium

I. Lardon (✉)
Department of Applied NMR and Laboratory for Systemic Physiological and Ecotoxicological Research (SPHERE), University of Antwerp, Groenenborgerlaan 171, 2020 Antwerp, Belgium
e-mail: isabelle.lardon@ua.ac.be

G. E. Nilsson · J. A. W. Stecyk
Department of Molecular Biosciences, University of Oslo, Blindernveien 31, 0316 Oslo, Norway

T. N. Vu · K. Laukens
Department of Mathematics and Computer Science, University of Antwerp, Middelheimlaan 1, 2020 Antwerp, Belgium

T. N. Vu · K. Laukens
Biomina-Biomedical Informatics Research Center Antwerp, Wilrijkstraat 10, 2650 Edegem, Antwerp, Belgium

## 1 Introduction

While the vast majority of vertebrates die almost instantly following anoxia exposure due to the failure of highly energy demanding tissues as the brain and heart, some species have evolved the ability to survive prolonged periods without oxygen (anoxia). This unusual capacity reveals that evolution has solved the problems of anoxia tolerance, an achievement that has eluded biomedical science. The best-studied examples of anoxia tolerant vertebrates are some North American freshwater turtles (Genera

*Trachemys* and *Chrysemys*) and a few fish including the crucian carp (*Carassius carassius*) and the congeneric goldfish (*Carassius auratus*) (Bickler and Buck 2007). In contrast to the crucian carp, the related common carp (*Cyprinus carpio*) survives severe hypoxia only for hours (at 15 °C) to 1 day (at 5 °C) (Stecyk and Farrell 2002).

Crucian carp are capable of surviving 1 or 2 days of anoxia at room temperature and several months during winter (Vornanen et al. 2009, for review). In order to tolerate such extreme environmental conditions, a coordinated balance between energy (ATP) demand and supply must be maintained, especially in the metabolically active brain and heart. The anoxic crucian carp utilizes a combination of two strategies to balance ATP supply and demand and thus survive prolonged anoxia: the increase of the anaerobic glycolytic ATP production (Pasteur effect) and the reduction of ATP consumption (metabolic depression) (Lutz and Nilsson 1997). The latter involves both behavioural and cellular adjustments, and for the closely related goldfish a 70 % depression of metabolic rate has been measured during anoxia (Van Waversveld et al. 1989). Still, anoxic crucian carp retain full cardiac output (Stecyk et al. 2004), and also brain function (Nilsson and Lutz 2004), although vision is suppressed (Johansson et al. 1997). Cellular adjustments to anoxic stress include increased levels of inhibitory amino acids neurotransmitters (GABA, glycine), combined with decreased levels of the excitatory neurotransmitter glutamate in order to mediate the lowering of the brain activity and, thus, energy consumption during anoxia (Nilsson and Lutz 1991; Hylland and Nilsson 1999). Simultaneously, energy demands are met by the massive liver glycogen store, the largest ever found in vertebrates (Nilsson 1990; Vornanen et al. 2009). This glycogen is needed to maintain the glycolytic ATP production during prolonged periods of energy distress. Additionally, lactate/$H^+$ self-poisoning, due to a higher anaerobic metabolic activity, is almost absent in crucian carp due to their exotic ability to transform lactate into ethanol in the muscles (Shoubridge and Hochachka 1980; Nilsson 1988).

Metabolomics permits insights into the dynamic biochemical processes of living systems at a certain point in time. For example, nuclear magnetic resonance has proven to be a key tool to study the metabolic profiles of complex biofluids in/from humans and animals (Lindon et al. 1999), neuronal tissues of humans (Cheng et al. 1997) and tissue extracts of mammals and fish (Coen et al. 2003; Kullgren et al. 2010). In the present paper, high resolution proton nuclear magnetic resonance ($^1$H-NMR) was applied to study the effects of anoxia exposure (24 h and 1 week) and subsequent reoxygenation (1 week) on the metabolomics of cold-acclimated (5 °C) crucian carp in order to lend insight into its anoxia survival mechanisms. We focused on the brain and the heart, the organs that normally show the highest sensitivity to oxygen deprivation, as well as on the liver and muscle due to their roles in glycogen storage and ethanol production, respectively. The NMR spectra of the different exposure groups were investigated using chemometric tools for pattern recognition, including principal component analysis (PCA) and partial least squares discriminant analysis (PLS-DA). Our results not only confirm known metabolic changes in tissues of anoxic crucian carp but also demonstrate the ability of $^1$H-NMR to discover hitherto unrecognized metabolic adjustments.

## 2 Materials and methods

### 2.1 Fish exposure and sampling

Sampling of crucian carp (*Carassius carassius*) tissues was conducted at the Department of Molecular Biosciences, University of Oslo, Oslo, Norway. All exposure protocols were performed in adherence with the regulations of the Norwegian Animal Health Authority and approved by the animal ethics authority at the University of Oslo.

Forty crucian carp of both sexes and with a mean body mass of 26.7 ± 14.0 g (mean ± S.D.) and a mean body length of 11.5 ± 2.5 cm (mean ± S.D.) were utilized. Fish were captured from a local pond in Oslo (Tjernsrud) and acclimated to 5 °C for at least 2 months prior to experimentation in tanks continuously supplied with aerated and dechlorinated Oslo tap water. Fish were maintained under a 12:12 h L:D photoperiod and fed daily with commercial carp food (Tetra Pond sticks, Tetra, Melle, Germany), but were not fed during the experimental period.

Four exposure groups of ten fish were examined: 1 week control normoxia, 24 h anoxia, 1 week anoxia and 1 week anoxia followed by 1 week normoxic recovery. Exposures were performed in flow-through (2–4 l/h) circular 25 l tanks (ten fish in each) submerged in a 5 °C large water bath wherein the fish were left to acclimate for 24 h in the dark prior to experimental onset. For anoxia, the tanks were sealed and the flow through water bubbled with nitrogen gas. Water oxygen levels and temperature were continuously recorded with an oxygen electrode (WTW oxi 3400i, Weilheim, Germany) connected to a computer. Water conditions considered anoxic (<0.01 mg O$_2$/l) were reached within 3 h. For control normoxia and reoxygenation, the flow-through water was bubbled with air.

At the conclusion of the exposure, fish were stunned by a sharp blow to the head, the spinal cord severed and tissues sampled. During tissue-sampling, the water in the anoxic tank was continuously nitrogen-gassed to ensure anoxic conditions for the remaining fish in the container. Four tissues were collected from each fish in the following order: brain, heart, liver and white muscle. All samples were

immediately snap-frozen in liquid nitrogen and stored at −80 °C until further analysis at the University of Antwerp (Departments of Chemistry and Biology), Belgium.

## 2.2 Tissue extraction procedure: methanol/chloroform/ water method (ratio 2/1/1.8)

Extraction of metabolites from tissues is often the most labour-intensive and rate-limiting step in metabolomics. Therefore, a deliberate, rapid, straightforward and reproducible tissue extraction technique is critical to achieve accurate profiles of the metabolome of an organism. For this reason, we evaluated several extraction strategies for fish tissues and eventually elected the methanol/chloroform/water technique (paper submitted to the Journal of Analytical Sciences) described by Lin et al. (2007) and Wu et al. (2008). The latter extraction method resulted in two separate fractions containing the hydrophilic (polar) and the hydrophobic (apolar) metabolites, respectively.

Frozen tissues were ground in a liquid nitrogen-cooled mortar and pestle and approximately 100 mg of homogeneous tissue powder was used for the extraction procedure. Ice cold methanol (4 ml per gram of tissue; analaR normapur, min. 99.8 %, VWR, Pennsylvania, USA) and ice cold milliQ water (0.85 ml/g) were added to the powder and the homogenate was vortexed for 1 min. Polar organic solvents such as methanol are typically mixed with water to extract hydrophilic metabolites (Coen et al. 2003; Stentiford et al. 2005). Subsequently, ice cold chloroform (4 ml/g; normapur, 99.3 %, VWR, Pennsylvania, USA) and milliQ water (2 ml/g) was added to extract the hydrophobic metabolites; the mixture was vortexed for 1 min and then incubated on ice for 10 min to partition. The supernatant was then centrifuged at 4 °C for 10 min at $2,000 \times g$, resulting in a biphasic solution. The upper polar and lower nonpolar layers were carefully removed and transferred to 15 ml sterile Falcon tubes. Subsequently, all samples were lyophilized overnight to avoid the presence of a dominant water signal in the ¹H-NMR spectra. Only the results of the polar fractions of brain, heart, liver and white muscle are discussed in the present study.

Prior to ¹H-NMR measurement, the polar tissue extracts were dissolved in 580 μl of sodium phosphate buffer prepared in $D_2O$ to minimize variations in sample pH and allow for deuterium locking, containing sodium-3-trimethylsilylpropionate (TMSP) as an internal standard (see following paragraph). Finally, the resulting samples were transferred to a 5 mm NMR tube (NE-HP5-7, Cortecnet, France) and analyzed immediately by ¹H-NMR.

The 50 mM sodium phosphate buffer in $D_2O$ (99.9 atom% D) consisted of $Na_2HPO_4$, 33.5 mM (AnalaR Normapur); $NaH_2PO_4$, 16.45 mM (GPR rectapur) (all from Merck, Darmstadt, Germany); 0.1 mM TMSP (≥98 %, Cambridge Isotope Laboratories, MA, USA); 0.5 mM

sodium azide (99 %, Acros Organics, NJ, USA). Deuterium chloride in $D_2O$ (ClD, >99 atom% D, 20 wt%) and sodium deuteroxide in $D_2O$ (NaOD, >99 atom% D, 40 wt%) (both from Acros Organics, NJ, USA) were added to achieve a pH of ∼7.

## 2.3 ¹H-NMR-based metabolomics of brain, heart, liver and white muscle extracts

Tissue extracts of crucian carp were analyzed on a Bruker Avance II-700 NMR spectrometer, operating at 700.13 MHz (Bruker Biospin, Europe), equipped with a 5 mm inverse TXI-Z probe and a BACS-60 automatic sample changer. Tuning, matching and shimming were performed automatically for each sample in order to minimize the variation due to sample manipulation.

One-dimensional ¹H-NMR spectra of brain, heart, liver and muscle extracts were acquired at 25 °C with a standard sequence using a 90° pulse (pulse sequence *zgpr*), a relaxation delay of 1.0 s with water presaturation, 64 scans collected into 16 k data points, a spectral width of 14 kHz and an acquisition time of 0.57 s per sample. Prior to Fourier transformation, all datasets were zerofilled to 32 k points and exponential line broadenings of 0.3 Hz were applied as well. Finally, all spectra were phase and baseline corrected and chemical shifts were referenced to TMSP (0.0 ppm) using the Topspin software (version 2.1, Bruker Biospin).

In order to confirm the metabolite identities, the spectra were compared to in-house and public databases and, additionally, to the results of 2D NMR experiments.

An overview of all metabolites, per tissue, that were discovered by ¹H-NMR in this study is provided in the Supplemental Materials.

## 2.4 Pre-processing of NMR data

The 1D spectra were converted to an appropriate format for statistical analysis by automatically segmenting each spectrum in 0.05 ppm integrated spectral regions (bins or buckets) between 0.5 and 10 ppm using AMIX (Analysis of Mixtures, version 3.8.5, Bruker Biospin). Buckets from 4.70 to 5.0 ppm, containing the residual water resonance, were excluded. All spectra were mean-centered and were normalized to total intensity in order to reduce the influence of concentration variability among the samples.

## 2.5 Statistical analyses

### 2.5.1 Univariate analysis

The generated bucket tables of the four tissue extracts were exported as a spread sheet to Excel (Microsoft Office Excel

2007) and a two-way analysis of variance (ANOVA), followed by a Benjamini–Hochberg test (Benjamini and Hochberg 1995) to counter the effect of multiple testing, were applied in R (version 2.9.2) to identify the buckets/metabolites that differed significantly between the control and the exposed fish. In all instances, $p < 0.05$ was used as the level of significance. Furthermore, in order to investigate whether these buckets also differed significantly between the different exposure groups, a student's $t$ test in excel followed by a Benjamini–Hochberg correction test in R were applied. In this case, $p < 0.05$ was applied as the level of statistical significance.

### 2.5.2 Multivariate analysis: pattern recognition techniques

The pre-processed NMR spectra were analysed by PCA using AMIX, to reduce the dimensionality of the data and to obtain an overview by showing trends, clusters and potential outliers within the data sets. Data points were considered as outliers when they were not situated within the 95 % confidence ellipse (Hotelling $T^2$ multivariate profiling) (Lindon et al. 2007).

In addition, to cope for the unsupervised nature of PCA, partial least squares for linear discriminant analysis (PLS-DA) was employed using AMIX. This supervised classification technique attempts to separate the samples according to their class membership, based on the linear combination of the original input variables, in such a way that an optimal inter-class separation is achieved. The obtained scores plots reveal the separation between the samples based on their class membership. The retrieved loadings plots offer insights in the variables responsible for the observed separation. The classification accuracy of the PLS-DA model was determined by leave-one out cross-validation using R to avoid overfitted results. The double cross-validation (2CV) strategy and permutation tests, described by Westerhuis et al. (2008) were applied on the data to estimate the quality of the developed PLS-DA model. The data points were randomly divided into 5 fractions, of which one was used for testing and the others for training and validating. Leave-one-out (LOOCV) according to Kohavi (1995) was used to select the optimal model. The data were randomly ordered 100 times and the average of the area under the ROC curve (AUROC) was used as the criteria. The optimal number of PLS-DA components was selected by trying different numbers, from one to the number of samples. The number of misclassification and the Q2 value were collected for the permutation test. A distribution was generated for the H0 hypothesis that no difference exists between the two classes. In the permutation test, the class labels of case and control are permutated and randomly assigned to different individuals.

With 'wrong' class labels, a classification model is calculated again. The data were permutated 1,000 times, and of each permutated set, the cross validation was repeated 20 times. The average parameter values were then computed.

A summary of the results of the PLS-DA double cross-validation strategy in all tissues is provided in the Supplemental Materials.

### 2.5.3 Hierarchical cluster-based peak alignment algorithm (CluPa)

As mentioned before, all $^1$H-NMR spectra of the different tissues were automatically segmented in 0.05 ppm integrated spectral regions (bins or buckets) between 0.5 and 10 ppm. As a consequence of this bucketing method, metabolites with similarly chemical structures (i.e. displaying NMR peaks at approximately identical resonance frequencies), but which exert a different metabolic function in organisms, were 'trapped' in a bucket of 0.05 ppm. In this study, this occurred for phosphocreatine and creatine metabolites in muscle and liver data sets.

In order to differentiate the phosphocreatine and creatine metabolites and their significant changes following anoxia exposure, a hierarchical Cluster-based Peak Alignment algorithm (CluPa) was applied on the liver and muscle data. A detailed description of the CluPa workflow for alignment and quantification on NMR spectra can be found in the original paper of Vu et al. 2011. Briefly, the CluPa alignment consists of four major steps which are integrated in one pipeline. First, instrumental noise is reduced/eliminated and peaks are collected from the NMR spectra by peak picking approaches. The method of continuous wavelet transform (CWT) is applied to detect the peaks in NMR spectra. Secondly, a representative reference spectrum is chosen to be a template for the alignment of the other spectra. Thirdly, the hierarchical cluster-based peak algorithm is applied to align a target spectrum to the reference spectrum. This is accomplished in a top-down fashion by building a hierarchical cluster tree from peak lists of reference and target spectra and then dividing the spectra into smaller segments based on the most distant clusters of the tree. Briefly, CluPa first performs the alignment on the whole spectrum and subsequently, CluPa splits the segment(s) of previous steps into smaller segments and applies an individual alignment shift to each of these. The last step includes the quantitative analysis. In our approach, an analysis of the data, based on the ratio of the between-group to within-group sums of squares (BW ratio) is performed for each data point in the NMR spectra. This ratio is related to the F-statistic or one-way ANOVA.

The results of the CluPa analysis in liver and muscle data sets are provided in the Supplemental Materials.

**Table 1** Identified metabolites, resulting from the two-way-ANOVA and Benjamini–Hochberg analysis ($p < 0.05$) in brain, heart, muscle and liver tissues

| Brain | Heart | Muscle | Liver |
| --- | --- | --- | --- |
| Valine/(iso)leu | Valine/(iso)leu | Valine/(iso)leu | Valine/(iso)leu |
| β-hydroxybutyric acid | β-hydroxybutyric acid | β-hydroxybutyric acid | β-hydroxybutyric acid |
| Lactate | Lactate | Lactate | Glutamate |
| Glutamate | Acetate | Acetate | Glutamine |
| Glutamine | Myo-inositol | Glutamate | (Phospho)creatine |
| GABA | Glycine | Glutamine | Glucose |
| NAA | Glucose | Taurine | Glycogen |
| | Alanine | Glucose | Glycine |
| | Glutamate | Glycine | ATP/ADP |
| | ATP/ADP | ATP/ADP | |
| | Formate | Formate | |
| | | (Phospho)creatine | |

The CluPa analysis enabled the differentiation of phosphocreatine and creatine in liver and muscle extracts and additionally, by consulting the results of the individual student's $t$ tests, it was possible to find out whether PCr levels decreased or increased as a consequence of 1d and/or 1w of anoxia and/or upon normoxic reoxygenation in these tissues.

## 3 Results

### 3.1 ^{1}H-NMR spectroscopy and statistical analyses of polar brain extracts

The ^{1}H-NMR spectra of polar brain extracts displayed a substantial amount of various metabolites. For example, the metabolites lactate, alanine, glucose, myo-inositol and ß-hydroxybutyric acid constituted some of the most intense resonances in those proton spectra. Consequently, the polar NMR spectra of all exposure groups provided a comprehensive insight in the metabolic composition of the crucian carp brain.

#### 3.1.1 Univariate analysis

Table 1 represents the results of the ANOVA analyses with Benjamini–Hochberg correction test of brain, heart, muscle and liver extracts, which exposed the buckets (metabolites) that differed significantly ($p < 0.05$) between the normoxic controls and the three exposure groups (1 day and 1 week of anoxia and 1 week normoxic recovery). These significant buckets were identified as beta-hydroxybutyric acid, NAA, GABA, glutamate and glutamine, lactate and valine/ (iso)leucine. Additionally, a student's $t$-test and Benjamini–Hochberg correction test ($p < 0.05$) were performed to find out whether these buckets also changed significantly between the various exposure groups. In order to have an

idea about the dynamic behaviour of the metabolites among the different exposure groups, box plots of the brain metabolites (Fig. 1) were created.

Compared to the normoxic controls, 24 h anoxia resulted in an increase in valine/(iso)leucine, lactate and GABA combined with a decrease in the concentrations of glutamate and glutamine. One week of anoxia resulted, compared to the normoxic controls, in an increase in valine/ (iso)leucine, beta-hydroxybutyric acid, lactate and GABA; with beta-hydroxybutyric acid and GABA being higher than after 24 h of anoxia. Contrarily, 1 week of anoxia caused a decrease in glutamate, glutamine and NAA; with glutamate, glutamine and NAA being lower than after 24 h of anoxia. Furthermore, reoxygenation resulted in a recovery of valine/(iso)leucine, NAA, GABA, lactate, glutamine and glutamate. Lactate and glutamate even displayed significant elevated levels in the recovered group, compared to the controls. Contrary, 1 week of normoxic recovery was too short to recover completely for the levels of beta-hydroxybutyric acid, compared to the controls.

Figure 2 visualizes the metabolic changes in polar brain extracts of crucian carp exposed to 24 h or 1 week anoxia and subsequent to 1 week of normoxic recovery.

#### 3.1.2 Multivariate analysis

In addition to the univariate statistical analysis, the 1D brain spectra of the four experimental groups were analyzed using unsupervised PCA and no outliers were detected. The results of the PCA analysis of brain, heart, liver and muscle data can be found in the Supplemental Materials.

In addition, a PLS-DA model for all exposure groups was constructed and the corresponding scores plot (Fig. 3) illustrates the separation of the different treatment groups: normoxic controls can be distinguished from the 24 h and 1 week anoxia group, and the recovered class. Moreover, a clear separation of the anoxic groups (24 h and 1 week) and
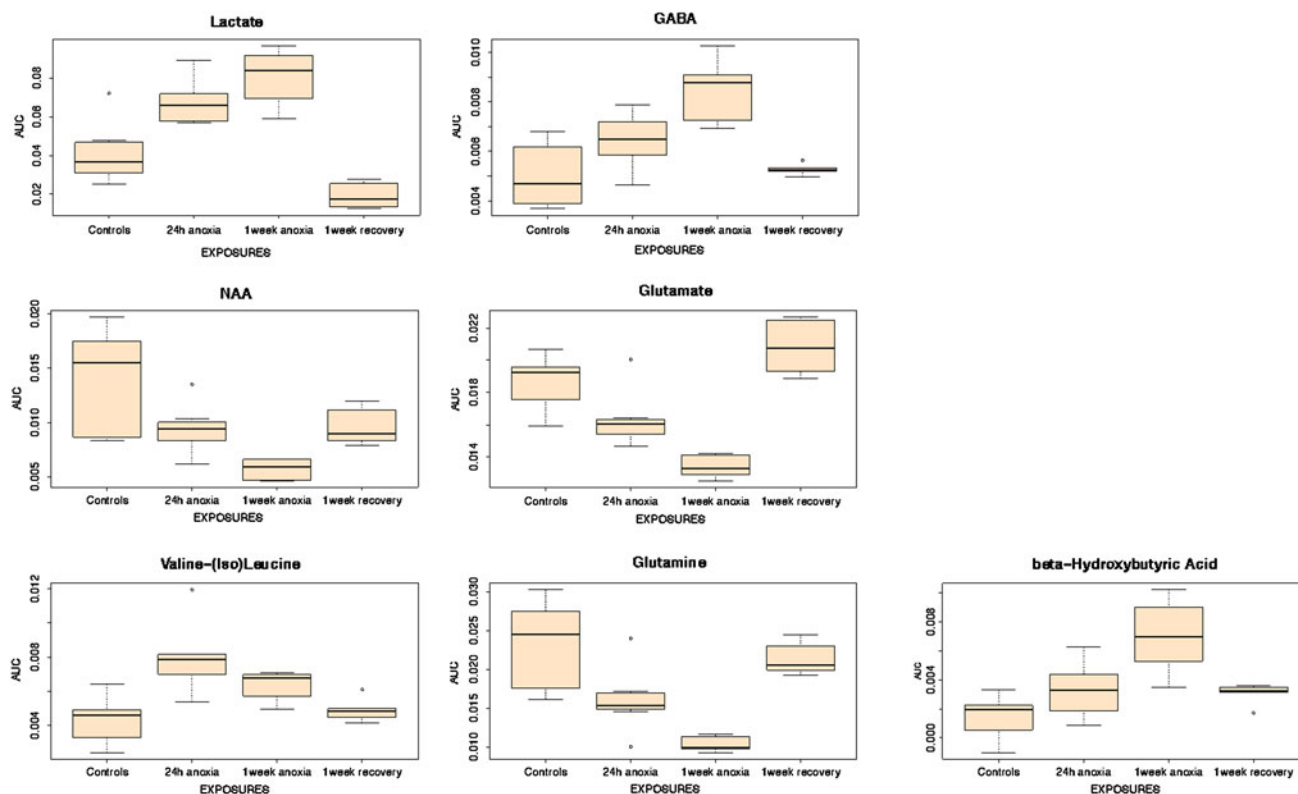
**Fig. 1** Box plots of polar brain data to visualize the buckets/metabolites that differed significantly ($p < 0.05$) between the control and exposure groups and between the individual exposure groups, identified by student's *t*-tests and two-way ANOVA analysis followed by Benjamini–Hochberg correction tests. The vertical axis of each box plot represents the AUC or Area Under the Curve intensities. The horizontal axis displays the four experimental groups: normoxic controls, 24 h anoxia, 1 week anoxia and 1 week recovery. The box plot is characterized by the five-number summary: the sample minimum (the smallest observation), the first or lower quartile (Q1), the median (vertical black line, Q2), the third or upper quartile (Q3) and the sample maximum (the largest observation). An *a* indicates a significant difference between exposed ($N = 19$) and control fish ($N = 7$) (*a* $p < 0.05$, *aa* $p < 0.01$, *aaa* $p < 0.001$), *b* indicates a significant difference between 24 h ($N = 7$) and 1 week anoxic fish ($N = 6$) (*b* $p < 0.05$, *bb* $p < 0.01$, *bbb* $p < 0.001$)

the normoxic groups (controls and recovered) can be observed (along PLS 1). Secondly, the PLS-DA loadings plot revealed the significant metabolites, responsible for the observed separation of all exposure groups and these observations confirmed the results of the univariate analysis.

Table 2 represents the average relative concentrations (mM) of the observed metabolites in polar brain extracts. The quantification of metabolites was performed through integration of the spectra, relative to the TMSP resonance at 0 ppm (0.1 mM).

## 3.2 $^1$H-NMR spectroscopy and statistical analyses of polar heart extracts

### 3.2.1 Univariate analysis

Table 1 illustrates the results of the ANOVA analyses with Benjamini–Hochberg correction of polar heart extracts. The significant ($p < 0.05$) buckets resulting from these analysis were identified as acetate, ATP/ADP, beta-hydroxybutyric acid, formate, glucose, glycine, lactate, myo-inositol and

valine/(iso)leucine. The box plots of the significant heart metabolites are shown in Supplemental Materials.

Compared to control normoxia, 24 h anoxia resulted in a significant increase in lactate, beta-hydroxybutyric acid and valine/(iso)leucine and a decrease in ATP/ADP. One week of anoxia resulted, compared to the normoxic controls, in an increase in lactate, beta-hydroxybutyric acid and valine/(iso)leucine. In contrast, compared to the normoxic controls, 1 week of anoxia caused a decrease in ATP/ADP, glucose, glycine, myo-inositol, formate, glutamate and acetate; with formate, glutamate, myo-inositol, and glycine being lower than after 24 h of anoxia.

Furthermore, reoxygenation resulted in a complete recovery to the control normoxic levels for valine/(iso)leucine, lactate, beta-hydroxybutyric acid, acetate, myo-inositol, glycine, glucose, ATP/ADP and formate.

### 3.2.2 Multivariate analysis

PCA was carried out to detect potential outliers in the polar heart data sets. Two data points were classified as outliers,

**Fig. 2** Schematic overview of the metabolic changes in polar brain extracts of crucian carp exposed to anoxia (24 h or 1 week) and subsequent 1 week reoxygenation. Increased metabolites are indicated by the symbol *upwards arrow* and decreasing metabolites are indicated by the symbol *downward arrow*. Key to metabolite abbreviations: Valine/Isoleu/Leu, valine/isoleucine/leucine; NAA, *N*-acetylaspartate, GABA, gamma-aminobutyric acid
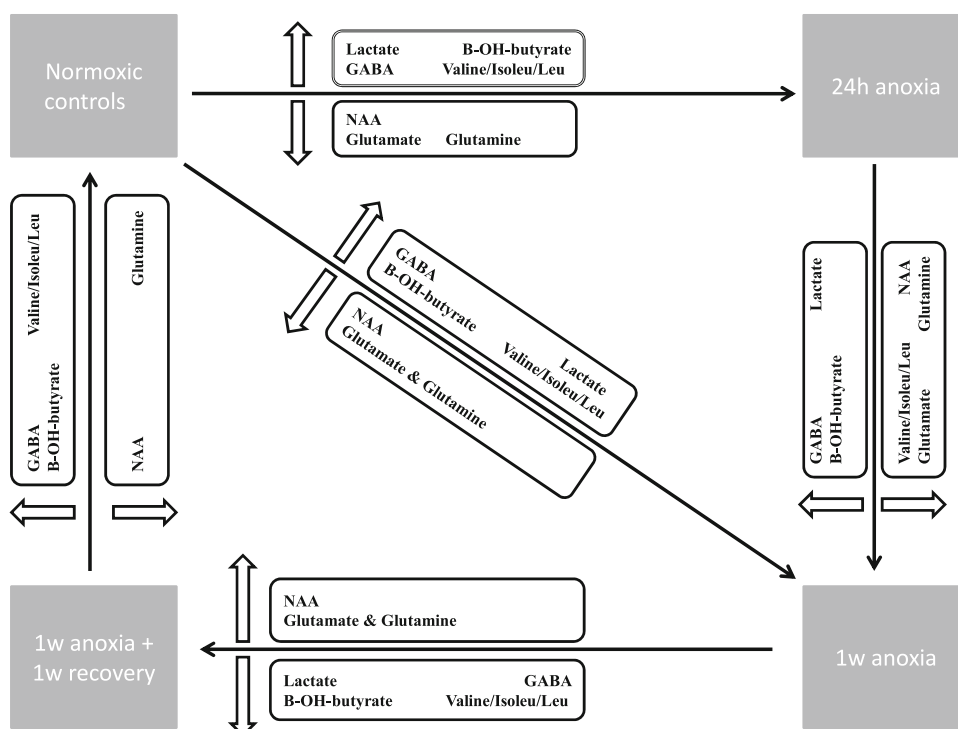


**Fig. 3** PLS-DA analysis tool to classify the different treatment groups in brain, based on their metabolic profiles. PLS-DA scores plot of ^{1}H-NMR spectra from polar brain extracts to illustrate the separation of the normoxic control group (*black circle*), N = 7, the 1 day anoxia group (*plus sign*), N = 7, the 1 week anoxia group (*open triangle*), N = 6 and the 1 week normoxic recovery group (x), N = 6 according to the first PLS-component in the X-axis (PLS 1) and the second PLS-component (PLS2) in the Y-axis
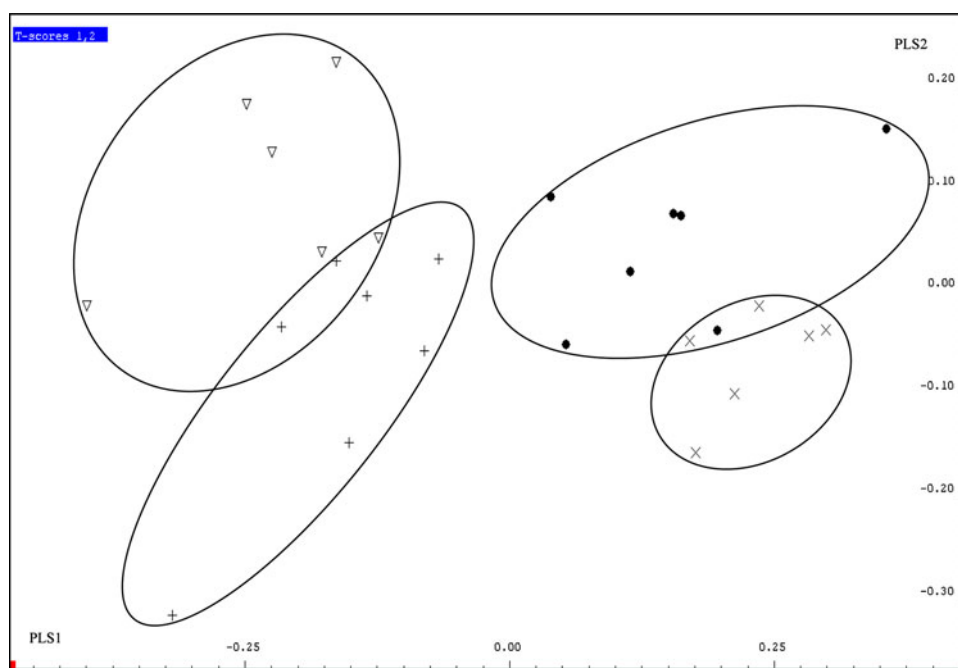


more specifically two spectra of the 1 week anoxic group. When these spectra were reviewed, a distorted baseline was identified as the cause for this aberrant behaviour and these samples were not included for further analyses.

Secondly, PLS-DA was performed to detect which variables carry the class distinguishing information.

The separation of the different groups in the four-class PLS-DA model was adequate in the equivalent scores plot. Furthermore, the results of the corresponding loadings plot

confirmed the identity of the metabolites which were detected by univariate analysis.

### 3.3 ^{1}H-NMR spectroscopy and statistical analyses of polar liver extracts

A typical 700 MHz ^{1}H-NMR spectrum of a normoxic polar liver extract using a standard water resonance presaturation pulse sequence is shown in Fig. 4a. In order to demonstrate

**Table 2** An overview of the average relative concentrations (mM) and SEM of observed metabolites in polar brain extracts

| | Controls | 1 day anoxia | 1 week anoxia | 1 week recovery |
|---|---|---|---|---|
| Acetate | 0.92 ± 0.18 | 1.74 ± 0.44* | 1.17 ± 0.19 | 0.88 ± 0.13 |
| ATP/ADP | 0.76 ± 0.11 | 1.21 ± 0.27* | 0.81 ± 0.12 | 0.83 ± 0.11 |
| GABA | 0.58 ± 0.10 | 1.70 ± 0.42* | 2.14 ± 0.31* | 0.60 ± 0.09 |
| Glutamate | 2.18 ± 0.33 | 4.10 ± 1.01* | 2.14 ± 0.36 | 2.42 ± 0.27 |
| Glycine | 0.20 ± 0.02 | 0.32 ± 0.06* | 0.31 ± 0.03* | 0.20 ± 0.02 |
| Lactate | 2.09 ± 0.24 | 7.58 ± 1.81* | 6.51 ± 0.70* | 1.05 ± 0.18 |
| Phosphocreatine | 2.39 ± 0.37 | 4.36 ± 0.93 | 3.16 ± 0.34 | 2.10 ± 0.34 |

Metabolites were quantified relatively to the TMSP resonance at 0 ppm (0.1 mM)

* The significant differences from the controls

all metabolites, spectral enlargements are presented in Fig. 4b (0–3 ppm), c (3–5 ppm), d (5.2–8.6 ppm).

### 3.3.1 Univariate analysis

Table 1 displays the results of the univariate analysis in polar liver extracts ($p < 0.05$). The significant buckets include phosphocreatine, ATP/ADP, glutamine, glutamate, glycogen, glycine, glucose, beta-hydroxybutyric acid and valine/(iso)leucine. The box plots of significant liver metabolites are provided in Supplemental Materials.

In comparison to normoxic controls, 24 h anoxia resulted in a decrease in phosphocreatine, ATP/ADP, glutamine, glutamate and glycogen, combined with an increase in glycine, glucose, valine/(iso)leucine and beta-hydroxybutyric acid. Subsequently, 1 week anoxia led to a decrease in ATP/ADP, glycogen, phosphocreatine, glutamate and glutamine, compared to normoxic controls; with ATP/ADP and glucose being significantly lower than after 24 h of anoxia. In contrast, after 1 week anoxia, glycine, valine/(iso)leucine and beta-hydroxybutyric acid were increased compared to the controls; with glycine, valine/(iso)leucine and beta-hydroxybutyric acid being significantly higher than the 24 h anoxia group.

Reoxygenation resulted in a complete recovery of the levels of phosphocreatine, glycine, glutamate, glutamine, glucose, valine/(iso)leucine, ATP/ADP and glycogen to the control levels. On the other hand, beta-hydroxybutyric acid displayed a higher level compared to the normoxic controls.

### 3.3.2 Multivariate analysis

PCA was used to examine all liver data of the four exposure groups. In total, five samples were considered as outliers (due to technical variation in the measurement of the spectra) and removed from further analyses.

Subsequently, a four-class PLS-DA model was used to discriminate the samples according to their class membership as described above. The scores plot of liver data in the Supplemental Materials illustrates an adequate separation of all exposure groups. In particular, a clear separation of the normoxic groups (controls and recovered ones) and the anoxic groups (1 day and 1 week) can be observed along the first PLS-DA component (PLS 1).

Additionally, the metabolites that resulted from the PLS-DA loadings plot corresponded to the ones that were identified by univariate analysis.

### 3.4 ¹H-NMR spectroscopy and statistical analyses of polar white muscle extracts

The polar ¹H-NMR spectra of muscle extracts expose prominent resonances such as phosphocreatine/creatine, alanine, beta-hydroxybutyric acid, lactate and taurine. An example of a proton NMR spectrum of white muscle is shown in Supplemental Materials.

### 3.4.1 Univariate analysis

Table 1 shows the results of the univariate analysis in muscle data. These tests identified the significant ($p < 0.05$) buckets that differed between the controls and the exposures. The metabolites were identified as beta-hydroxybutyric acid, lactate, glycine, phosphocreatine, acetate, valine/(iso)leucine, ATP/ADP, glucose, taurine, glutamate, glutamine and formate. The box plots of these metabolites are provided in Supplemental Materials.

Compared to the normoxic status, 24 h anoxia resulted in a significant increase in the concentrations of beta-hydroxybutyric acid, lactate, glycine, acetate and valine/(iso)leucine, combined with a decrease in ATP/ADP, phosphocreatine, glucose and taurine. After 1 week of anoxia, beta-hydroxybutyric acid, lactate, glutamate, glutamine and valine/(iso)leucine were significantly increased, compared to the controls; with beta-hydroxybutyric acid, glutamine, taurine and valine/(iso)leucine being higher

**Fig. 4 a** One-dimensional 700 MHz ^{1}H-NMR spectrum (0–8.6 ppm) representing a polar liver extract of a normoxic control fish, analyzed with a standard 90° pulse sequence. Low intensity regions are illustrated by inset spectral enlargements from 0 to 3 ppm (**b**), from 3 to 5 ppm (**c**) and from 5.2 to 8.6 ppm (**d**). Key to peak assignments: (*a*) TMSP (internal standard), (*b*) Valine(Iso)Leucine, (*c*) beta-hydroxybutyric acid, (*d*) lactate, (*e*) alanine, (*f*) acetate, (*g*) glutamate, (*h*) glutamine (*i*) succinate, (*j*) aspartate, (*k*) unknown, (*l*) (phospho)creatine, (*m*) malonate, (*n*) phosphocholine, (*o*) taurine, (*p*) glucose, (*q*) glycine, (*r*) malate, (*s*) residual suppressed water resonance, (*t*) glycogen, (*u*) ATP/ADP, (*v*) fumarate, (*w*) oxypurinol, (*x*) formate
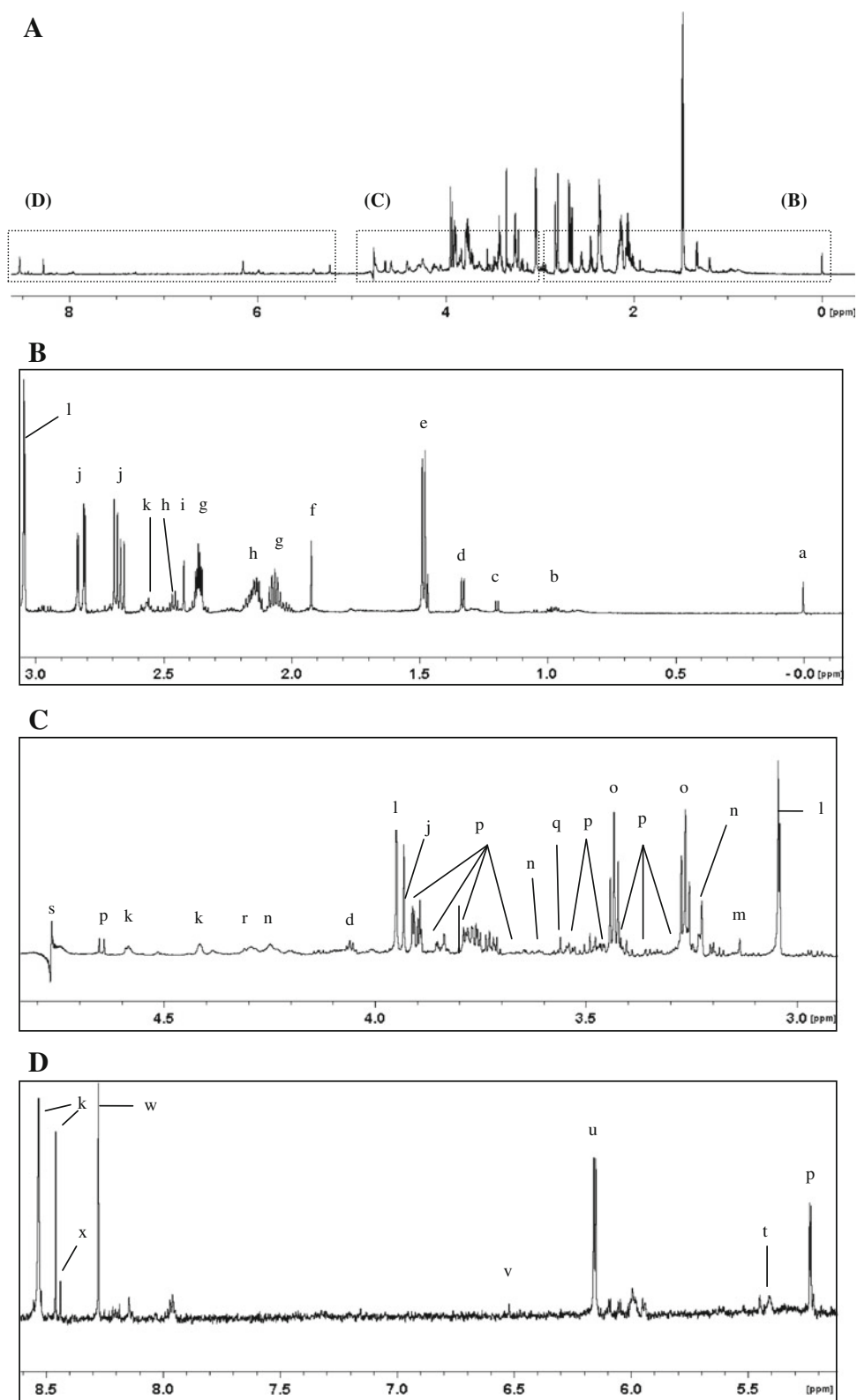


than the 24 h anoxia group. In contrast, 1 week of anoxia caused a significant decrease in phosphocreatine, ATP/ADP, glucose, formate, glycine and taurine, compared to the controls; with glucose, formate, glycine, acetate being lower than the 24 h anoxia fish. A complete recovery was present for valine/(iso)leucine, ATP/ADP, formate, lactate, glucose, glycine, taurine, beta-hydroxybutyric acid, glutamate, glutamine and acetate.

### 3.4.2 Multivariate analysis

The muscle spectra were subsequently analyzed by PCA and no outliers were detected in the different exposure groups. Following PCA, all datasets were submitted to the PLS-DA model in an attempt to discriminate the samples according to their class membership.

The PLS-DA scores plot of muscle extracts resulted in an adequate but less clear separation of the different exposure groups, compared to the scores plots of brain, heart and liver. Nevertheless, the corresponding loadings plot confirmed the metabolites identified by univariate analysis.

## 4 Discussion

In order to provide a transparent and comprehensive explanation for the achieved results in this study, the discussion is divided into three sections that respectively examine the metabolites affiliated with the general energy metabolism (e.g. glucose, lactate, ATP/ADP, etc.), the amino acids and neurotransmitters (glutamate, NAA, GABA, etc.) and finally, the role of previously unrecognized changing metabolites in anoxia exposed fish.

### 4.1 General energy metabolism

Under normoxic conditions, greater than 95 % of ATP is produced aerobically in vertebrate cells, whereby each mole of glucose is oxidized by 6 mol of $O_2$ to yield 36 mol of ATP (Lutz et al. 2003). In these aerobic conditions, most glucose is fully oxidized to $H_2O$ and $CO_2$. The net lactate production accounts for only a negligible (<4 %) part of the total glucose metabolized. In contrast, anoxia causes a dramatic shift from aerobic to anaerobic metabolism where sufficient ATP can only be generated by up-regulating $O_2$-independent mechanisms, namely anaerobic glycolysis and other metabolic pathways that rely on substrate-level phosphorylation. Eventually, glucose/glycogen and/or high-energy phosphates (metabolic fuels) become exhausted and metabolic waste products such as lactate and $H^+$ accumulate.

Remarkably, crucian carp withstand lactate self-poisoning due to their unique ability to convert lactate into ethanol, which is then lost to the environment across the gills by diffusion (Nilsson 1988; Vornanen et al. 2009). Ethanol was not detected in any tissues in this study. However, this might be due to the lyophilisation procedure, resulting in the evaporation of the volatile ethanol. An increase in lactate during anoxia was observed in the brain, heart and muscle. In the brain, the lactate increase was apparent already after 1 day of anoxic exposure and this

was at least as high after 1 week of anoxia. The lack of a major increase in lactate between 1 day and 7 days of anoxia shows that lactate was further metabolized to ethanol and was probably at a steady-state concentration.

A significantly increased lactate concentration was also present in the 1 week anoxic heart samples. Simultaneously, a decreased glucose concentration was observed when fish were exposed to 1 week of anoxia. However, we were not able to detect significantly changing lactate concentrations in anoxic livers but fluctuating glycogen and glucose concentrations were detected clearly during anoxia.

Short and long term anoxia caused a significant increase of glucose and a decrease of glycogen in liver extracts. Crucian carp has the largest glycogen store of all vertebrates (Vornanen et al. 2011) and the size of this carbohydrate deposits limits the hypoxia/anoxia tolerance of crucian carp. In contrast to liver tissue, no glycogen and thus no changes in the glycogen content of brain, heart and white muscle were observed in this study. In 2006, a study by Vornanen and Paajanen (2006) investigated the glycogen concentrations in crucian carp brains. Apparently, clear seasonal cycling patterns were observed with glycogen values ranging from 203.7 µM/g in February to 12.9 µM/g in July. Furthermore, another study by this group analyzed the size of glycogen stores in different tissues of crucian carp (Vornanen et al. 2011). Clearly, the highest mean glycogen content existed in the liver (18 % of wet weight) whereas lower glycogen levels were present in brain (3 %), muscle (2 %) and heart (2 %). Apparently, the glycogen concentration remains under the detection threshold in all tissues of this study except the liver. Increased sample sizes should overcome this problem, but brings some practical challenges, since the animals and consequently their organs are rather small.

Furthermore, 1 and 7 days of anoxia exposure resulted in a decrease of liver and muscle phosphocreatine concentrations. Phosphocreatine stores are, in addition to tissue glycogen stores, important energy reserves (particularly in muscle) by giving off the phosphate group to ADP to form ATP (Mandic et al. 2008).

All tissues, except for the brain, demonstrated a decrease in ATP in response to anoxia exposure but reoxygenation enabled a complete recovery. Compared to the normoxic controls, an increase of a ketone body, beta-hydroxybutyric acid, was observed in all 1 week anoxic tissues. This probably reflects the stop in ketone-body metabolism as the citric acid cycle is not functioning during anoxia.

### 4.2 Amino acids and neurotransmitters

Anoxia not only altered the cellular energy metabolism, it also influenced the amino acid and/or neurotransmitter

patterns. Specifically, the characteristic anoxia-induced features, i.e. an increased concentration of inhibitory compounds (GABA, glycine) combined with a decreased concentration of excitatory metabolites (glutamate, glutamine) were detected in the anoxic brain extracts (Nilsson et al. 1991).

GABA, a major inhibitory neurotransmitter in the adult vertebrate central nervous system and we observed an increase of brain GABA at 1 day of anoxia, and the increase was further noticed following 1 week of anoxia. Such an increase in GABA during periods of oxygen deficiency has previously been observed in crucian carp brain, both in tissue (Nilsson 1990) and extracellularly (Hylland and Nilsson 1999) and the metabolic pathways supporting GABA production and degradation are well characterized in vertebrate nervous tissues. The elevation of brain GABA is thought to be a main mechanism for anoxic metabolic depression.

As a consequence of the activation of inhibitory GABA receptors, the synaptic and electrical activities in the brain decrease and hence, the overall energy consumption is reduced. Moreover, GABA is synthesized from glutamate and the continued production of GABA at the expense of glutamate during anoxia could provide further depression of brain activity, since glutamate is the major excitatory neurotransmitter in vertebrates. Indeed, the concentrations of glutamate and the intimately connected glutamine (precursor and storage form of glutamate in the brain) decreased when carp were exposed to 1 day and 1 week of anoxia.

Glutamate and glutamine are non-essential amino acids of the citric acid cycle superfamily and can be transaminated into citric acid cycle intermediates within most cells (Podrabsky et al. 2007). Firstly, a decreased brain tissue glutamate level could be directly related to a decreased tricarboxylic acid cycle activity. However, studies are available, demonstrating an increase or a stabilization of glutamate in the liver and muscle of goldfish respectively (Van Waarde et al. 1982). Secondly, a more straightforward explanation is related to the similar increase of brain GABA after anoxia. Glutamate is the immediate precursor of GABA and the glutamate decarboxylase reaction, which converts glutamate to GABA, proceeds during anoxia. Hence, an increased GABA concentration in the brains of anoxic carp can be related to a decreased glutamate (and glutamine) concentration.

A significant decrease of N-acetylaspartate was present in the brain of 1–7 day anoxic fish. N-acetylaspartate is present almost exclusively in neurons/neuronal processes and is an important metabolite in brain. For instance, NAA is decreased in a variety of human neurodegenerative diseases associated with neuronal loss (Raman et al. 2005) and therefore, NAA can be considered as a marker of neuronal

density or viability. The decreased brain NAA in this study can be due to a decreased production of NAA in neurons and a possible loss of NAA from damaged neurons. Although crucian carp obviously are masters of anoxic survival, it cannot be excluded that anoxia leads to some neuronal damage or loss that is effectively repaired or restored upon reoxygenation. Secondly, NAA can act as a source of acetate, enabling the lipid and myelin synthesis in oligodendrocytes. Therefore, the decreased NAA concentration in brain may reflect an attempt to diminish the extent of cell membrane damage during anoxia. Thirdly, the enzyme responsible for the synthesis of NAA, acetyl-CoA-l-aspartate-N-acetyltransferase, is localized exclusively in the mitochondria (Choi et al. 2007). Accordingly, decreased NAA levels after anoxic periods may plausibly reflect an impaired mitochondrial energy production.

The branched-chain amino acids (BCAA) valine/isoleucine/leucine increased in all anoxic tissues. These essential amino acids are key molecules essential for regulating global growth and metabolism (Wang et al. 2011). Particularly leucine is important for heart muscle health and can stimulate protein synthesis, cellular metabolism and cell growth (Wang et al. 2011). In addition, isoleucine is both glucogenic as well as ketogenic (Voet and Voet 1995). In this study, the observed increase of the BCAA's can be due to the stop in oxidation by mitochondrial enzymes in anaerobic tissues. The increased concentration of BCAA can also be due to a reduced consumption of amino acids (protein synthesis suppression) or an increased catabolism in periods of anoxia (Podrabsky et al. 2007).

## 4.3 Novel metabolites

Lastly, the NMR study of anoxic tissue extracts introduced the appearance of compounds that are 'novel', i.e. previously unrecognized to play a role in the present context: myo-inositol in heart extracts and taurine in white muscle.

Myo-inositol decreased significantly in the heart of anoxic fish. So far, its exact function is not well understood, although it is believed to be an essential element for cell growth, an osmolite, a glial marker and a storage form for glucose (Govindaraju et al. 2000). Maybe, the decrease of myo-inositol in the heart extracts could reflect a change in the heart phosphoinositide-energy metabolism.

Taurine decreased significantly in muscle tissue. A first decrease of taurine was noticed after 24 h of anoxia and the concentration continued to decrease after 1 week of anoxia. This sulfonic amino acid is highly concentrated in fish tissue (skeletal muscle, heart, brain and retina) and has many important metabolic functions. In the anoxic crucian carp brain, it may act as an inhibitory neuromodulator, counteracting brain damage (Hylland and Nilsson 1999). Furthermore, taurine has antioxidative and membrane-

stabilizing properties, is a natural calcium antagonist and osmoregulator and is essential for the development and function of skeletal muscle (Schaffer et al. 2010). Additionally, it modulates the immune response, regulates the transport of ions, signal transduction, cell proliferation and DNA repair (Kuzmina et al. 2010). In this study, a decrease of taurine was noticed following 24 h and 1 week of anoxic stress. This decrease might be due to the augmented consumption of this polyfunctional and beneficial amino acid in anoxic muscles.

## 5 Concluding remarks

To conclude, the present study provides an excellent example of the usefulness of NMR-based metabolomics to examine the biochemical responses of aquatic animals to environmental challenges. We used $^1$H-NMR based metabolomics combined with chemometric tools, to explore the metabolic responses of crucian carp to anoxic stress.

Metabolic profiles of heart, brain, liver and muscle extracts confirmed previously observed changes in energy-related compounds, such as glucose and lactate, and in amino acid neuromodulators. Moreover and more importantly, the study also illustrates the potential of $^1$H-NMR based metabolomics to discover changes in the levels of metabolites that previously not received attention in the present context. These "novel" metabolites included myo-inositol and taurine in this case.

Further research in this unique fish model will undoubtedly lead to the identification of other novel and key elements involved in the mechanism of anoxia resistance.

## References

Benjamini, Y., & Hochberg, Y. (1995). Controlling the false discovery rate: A practical and powerful approach to multiple testing. *Journal of the Royal Statistical Society-Series B (Methodological), 57*(1), 289–300.

Bickler, P. E., & Buck, L. T. (2007). Hypoxia tolerance in reptiles, amphibians, and fishes: Life with variable oxygen availability. *Annual Review of Physiology, 69*, 145–170.

Cheng, L. L., Ma, M. J., Becerra, L., et al. (1997). Quantitative neuropathology by high resolution magic angle spinning proton magnetic resonance spectroscopy. *Proceedings of the National Academy of Sciences of the United States of America, 94*(12), 6408–6413.

Choi, J. K., Dedeoglu, A., & Jenkins, B. G. (2007). Application of MRS to mouse models of neurodegenerative illness. *NMR in Biomedicine, 20*, 216–237.

Coen, M., Lenz, E. M., Nicholson, J. K., et al. (2003). An integrated metabonomic investigation of acetaminophen toxicity in the mouse using NMR spectroscopy. *Chemical Research in Toxicology, 16*(3), 295–303.

Govindaraju, V., Young, K., & Maudsley, A. A. (2000). Proton NMR chemical shifts and coupling constants for brain metabolites. *NMR in Biomedicine, 13*(3), 129–153.

Hylland, P., & Nilsson, G. E. (1999). Extracellular levels of amino acid neurotransmitters during anoxia and forced energy deficiency in crucian carp brain. *Brain Research, 823*, 49–58.

Johansson, D., Nilsson, G. E., & Doving, K. B. (1997). Anoxic depression of light-evoked potentials in retina and optic tectum of crucian carp. *Neuroscience Letters, 237*(2–3), 73–76.

Kohavi, R. (1995). A study of cross-validation and bootstrap for accuracy estimation and model selection. *Proceedings of the Fourteenth International Joint Conference on Artificial Intelligence, 2*, 1137–1143.

Kullgren, A., Samuelsson, L. M., Forlin, L., et al. (2010). A metabolomics approach to elucidate effects of food deprivation in juvenile rainbow trout (*Oncorhynchus mykiss*). *American Journal of Physiology-Regulatory Integrative and Comparative Physiology, 299*(6), R1440–R1448.

Kuzmina, V. V., Gavrovskaya, L. K., & Ryzhova, O. V. (2010). Taurine. Effect on exotrophia and metabolism in mammals and fish. *Journal of Evolutionary Biochemistry and Physiology, 46*(1), 19–27.

Lin, C. Y., Wu, H. F., Tjeerdema, R. S., & Viant, M. R. (2007). Evaluation of metabolite extraction strategies from tissue samples using NMR metabolomics. *Metabolomics, 3*(1), 55–67.

Lindon, J. C., Nicholson, J. K., & Everett, J. R. (1999). NMR spectroscopy of biofluids. *Annual Reports on NMR Spectroscopy, 38*, 1–88.

Lindon, J. C., Nicholson, J. K., & Holmes, E. (2007). *The handbook of metabonomics and metabolomics* (1st ed.). Amsterdam: Elsevier.

Lutz, P. L., & Nilsson, G. E. (1997). Contrasting strategies for anoxic brain survival: Glycolysis up or down. *Journal of Experimental Biology, 200*, 411–419.

Lutz, P. L., Nilsson, G. E., & Prentice, H. M. (2003). *The brain without oxygen causes of failure-physiological and molecular mechanisms for survival. Mechanisms of Brain Anoxia Tolerance (3rd ed.)* (pp. 131–189). The Netherlands: Kluwer Academic Publishers.

Mandic, M., Lau, G. Y., Nijjar, M. M. S., & Richards, J. G. (2008). Metabolic recovery in goldfish: A comparison of recovery from severe hypoxia exposure and exhaustive exercise. *Comparative Biochemistry and Physiology, Part C, 148*, 332–338.

Nilsson, G. E. (1988). A comparative study of aldehyde dehydrogenase and alcohol dehydrogenase activity in crucian carp and three other vertebrates: Apparent adaptations to ethanol production. *Journal of Comparative Physiology B, 158*, 479–485.

Nilsson, G. E. (1990). Long term anoxia in crucian carp: Changes in the levels of amino acid and monoamine neurotransmitters in the brain, catecholamines in chromaffin tissue, and liver glycogen. *Journal of Experimental Biology, 150*, 295–320.

Nilsson, G. E., & Lutz, P. L. (1991). Release of inhibitory neurotransmitters in response to anoxia in turtle brain. *American Journal of Physiology, 261*(1), R32–R37.

Nilsson, G. E., & Lutz, P. L. (2004). Anoxia tolerant brains. *Journal of Cerebral Blood Flow and Metabolism, 24*(5), 475–486.

Nilsson, G. E., Lutz, P. L., & Jackson, T. L. (1991). Neurotransmittors and anoxic survival of the brain: A comparison between anoxia-tolerant and anoxia-intolerant vertebrates. *Journal of Physiological Zoology, 64*, 638–652.

Podrabsky, J. E., Lopez, J. P., Fan, T. W. M., Higashi, R., & Somero, G. N. (2007). Extreme anoxia tolerance in embryos of the annual

killifish *Austrofundulus limnaeus*: Insights from a metabolomics analysis. *Journal of Experimental Biology, 210*(13), 2253–2266.

Raman, L., Tkac, I., Ennis, K., et al. (2005). In vivo effect of chronic hypoxia on the neurochemical profile of the developing rat hippocampus. *Developmental Brain Research, 156*(2), 202–209.

Schaffer, S. W., Jong, C. J., Ramila, K. C., & Azuma, J. (2010). Physiological roles of taurine in heart and muscle. *Journal of Biomedical Science, 17*(1), 1–8.

Shoubridge, E. A., & Hochachka, P. W. (1980). Ethanol: Novel end product of vertebrate anaerobic metabolism. *Science, 209*(4453), 308–309.

Stecyk, J. A. W., & Farrell, A. P. (2002). Cardiorespiratory responses of the common carp (*Cyprinus carpio*) to severe hypoxia at three acclimation temperatures. *Journal of Experimental Biology, 205*(6), 759–768.

Stecyk, J. A. W., Stensløkken, K.-O., Farrell, A. P., & Nilsson, G. E. (2004). Maintained cardiac pumping in anoxic crucian carp. *Science, 306*, 77.

Stentiford, G. D., Viant, M. R., Ward, D. G., et al. (2005). Liver tumors in wild flatfish: A histopathological, proteomic, and metabolomic study. *OMICS: A Journal of Integrative Biology, 9*(3), 281–299.

Van Waarde, A., Van den Thillart, G., & Dobbe, F. (1982). Anaerobic metabolism of goldfish, *Carassius auratus* (L.). Influence of anoxia on mass-action ratios of transaminase reactions and levels of ammonia and succinate. *Journal of Comparative Physiology B-Biochemical, Systemic, and Environmental, Physiology, 147*(1), 53–59.

Van Waversveld, J., Addink, A. D. F., & van den Thillart, G. (1989). Simultaneous direct and indirect calorimetry on normoxic and anoxic goldfish. *Journal of Experimental Biology, 142*, 325–335.

Voet, D., & Voet, J. G. (1995). *Biochemistry* (Vol. 2). New York: Wiley.

Vornanen, M., Asikainen, J., & Haverinen, J. (2011). Body mass dependence of glycogen stores in the anoxia-tolerant crucian carp (*Carassius carassius L.*). *Naturwissenschaften, 98*, 225–232.

Vornanen, M., & Paajanen, V. (2006). Seasonal changes in glycogen content and Na$^+$-K$^+$-ATPase activity in the brain of crucian carp. *American Journal of Physiology: Regulatory, Integrative and Comparative Physiology, 291*, 1482–1489.

Vornanen, M., Stecyk, J. A. W., & Nilsson, G. E. (2009). The anoxia-tolerant crucian carp (*Carassius carassius L.*). *Fish Physiology, 27*, 397–441.

Vu, T. N., Valkenborg, D., Smets, K., Verwaest, K., Dommisse, R., Lemiere, F., et al. (2011). An integrated workflow for robust alignment and simplified quantitative analysis of NMR spectrometry data. *BMC Bioinformatics, 12*, 405.

Wang, Y., Haipeng, S., Lu, G., Ren, S., & Chen, J. (2011). Catabolism of branched-chain amino acids in heart failure: Insights from genetic models. *Pediatric Cardiology, 32*, 305–310.

Westerhuis, J. A., Hoefsloot, H. C. J., Smit, S., et al. (2008). Assessment of PLSDA cross validation. *Metabolomics, 4*(1), 81–89.

Wu, H. F., Southam, A. D., Hines, A., & Viant, M. R. (2008). High-throughput tissue extraction protocol for NMR and MS-based metabolomics. *Journal of Analytical Biochemistry, 372*(2), 204–212.